Energy and Thermofluids Engineering

Available at https://asps-journals.com

Heat transfer performance analysis through inline and staggered grooved microchannel using lattice Boltzmann method

R. Biswas[1,2], M. M. Rahman[2], A. Khanom[2], M. A. Taher[2]✉

1. Open School, Bangladesh Open University, Gazipur-1705, Bangladesh

2. Department of Mathematics, Dhaka University of Engineering & Technology, Gazipur-1707, Bangladesh

Received June 11, 2023

Revised June 23, 2024

Accepted July 29, 2024

Published online: September 22, 2024

Keywords

Heat Transfer

Inline and Staggered

Knudsen Number

Roughness Height

Grooved Microchannel

Abstract: The D2Q9 Bhatnagar-Gross-Krook (BGK) model, utilizing the Thermal Lattice Boltzmann Method (TLBM) to examine the temperature and mass transfer numerically across inline and staggered grooved microchannels. The conditions are (a) cold fluid at inlet and outlet, (b) walls are heated (c) relative roughness height is rh=4%, 8% and 12% according to channel height and (d) parabolic velocity profile at inlet and outlet section with slip flow at the walls for different Knudsen numbers from Kn=0.02 to 0.10. The study goals to examine the impact of temperature profiles, Nusselt number, average friction coefficients and performance analysis of smooth, inline and staggered grooved microchannels. The friction coefficient is defined as the ratio of the Poiseuille number (Pn) and Reynolds number (Re) and the dimensionless heat transfer recognized by the Nusselt number (Nu) has been studied to investigate the roughness effects of the surface. The result presented that the average friction increased gradually with the height of relative roughness and reduced significantly with growing Kn for both inclined and staggered grooved microchannels. In addition, compared to smooth, inline and staggered microchannels, the lowest friction occurred for smooth and the highest friction showed for inline grooved channels. The maximum average friction factor is depicted as 107.053 for inline grooved microchannels when rh=12% and Kn is 0.02. The extreme heat transfer rate is found to be 9.015 when the microchannel is smooth and Kn=0.02. The highest performance PE=1.013248 is exhibited by the staggered microchannel when Kn=0.02 and with rh=12%. Compared to the inline grooved channel, the staggered grooved microchannel has demonstrated better performance.

1. Introduction

Significant attention has been drawn to the roughness effect on fluid flow, temperature and mass transmission over the past few eras for its practical applications in the solar collectors, garments industry, pharmaceutical industry, electronic cooling industry, food processing, media sector, engineering, medicine, and materials science to create more efficient, sustainable, and effective technologies, renewable energy engineering etc. (Fábregas et al., 2022, Jafari et al., 2017; Walter et al., 2020; Qi et al., 2022; Zhao and Wang, 2019; Feng et al., 2018; Zhang et al. 2019; Harris et al, 2022; Aouissi et al., 2023; Abdelsalam and Zaher, 2023; Bhatti et al., 2023).

The roughness size and shape can have a vital effect on the fluid movement and heat transmission appearances in the microscale flow system. Therefore, friction considerably affects surface roughness for gas flow in a microchannel (Sahar et al., 2017; Taher et al., 2017; Biswas et al., 2015;

✉ Corresponding author. E-mail address: tahermath@duet.ac.bd

Chai et al., 2008; Ji et al., 2006, Yuan and Rahman, 2016) It was found that the roughness of the channel significantly influences the friction factor in laminar flow. Based on their research results, it was observed that the friction factor growths gradually with the rise of relative roughness, on the contrary, the friction factor reductions significantly with the rises of Knudsen number.

Examining flow disturbances at periodic intervals serves as a method to analyze both flow structure and the characteristics of heat transfer. Truly, it is a frequently used technique to comprise baffles in a channel along the streamwise way such as offset fins, louvers, communicating channels etc. This study also discussed the effect of liquid flow and temperature transfer applications as another controlling parameters (Taher et al., 2015; Boonloi and Jedsadaratanachai, 2022; Wang et al., 2020; Sharma et al., 2015; Kim et al., 2008; Taher et al., 2014). Nanofluids display higher thermal conductivity compared to conventional fluids at the nanometer size, due to the inclusion of metal nanoparticles. (Abdelsalam et al., 2023)

In this study, roughness effects on two-dimensional microchannels and rarefied gas flow behavior are simulated using LBM. To perform realistic hydrodynamics simulation customs a precise lattice model representing mathematical results of the alternative method of Navier-Stokes equations; Rovenskaya and Croce, 2016; He et al., 1998; Niu et al., 2007). The regional equilibrium distribution has been selected to recover the N–S macroscopic equations by the lattice Bhatnagar-Gross-Krook (LBGK) model (Liao and Jen, 2011; Mohamad, 2007; D'Orazio et al., 2004; Tan et al. 2022; Cao et al., 2006; Xu and Yan, 2023)

(Zhu et al, 2020) Microchannel heat sinks featuring rectangular grooves and various rib shapes have been the subject of investigation concerning temperature transfer and fluid movement. The results indicated that the rectangular ribs produce a beast overall performance. Analytical and experimental performances have been done by (Dahani et al., 2023) in the case of a circular block on a heated conjugate conduction-convection square cavity and the result obtained that the average Nusselt number inside a large cavity is affected by the presence of another block with large size and high conductivity.

The friction factor (f) is specified as the ratio of Poiseuille number (Pn) and Reynolds (Re) number. Generally, Pn increases with increased roughness due to the augmentation in near-wall velocity gradient for the gas flow. On the contrary, as the Kn increases, the Poiseuille number decreases due to a greater occurrence of velocity slip near the wall. Using the LBM, the effect of roughness has been discussed regarding the Poiseuille number by (Rovenskaya and Croce, 2016; Liue et al., 2011; Taher et al., 2022a,b; Chen and Tian 2009).

(Tan et al., 2022) conducted for gas-liquid mass transfer by a phase-field the LBM and outcomes show that a source term is generated and added to the phase field to represent the volume change caused by mass transfer.

The objectives of the study are to improvement a fundamental considerate of the effect of grooved on fluid velocity and temperature profile, Nusselt number, average friction coefficient and performance analysis for separate flow conditions regarding different surface roughness with Knudsen numbers in microchannels using an alternative Thermal Lattice Boltzmann Method (TLBM). From the above literature, we found that many studies have used TLBM for fluid flow problems. According to the researchers' knowledge, the TLBM has not yet conducted a comparative study of smooth, inline and staggered microchannel problems with varying relative roughness heights.

The present study investigates the effect on the velocity and temperature profiles, friction coefficient and performance enhancement for different flow conditions in grooved inline and staggered microchannels according to the relative roughness height is rh = 4%, 8% and 12% in terms of channel height and various Kn=0.02, 0.05 and 0.10 which represent the slip flow regime. Moreover, to examine the contemporary effect of temperature transfer and rubbing properties using the LBM and compare to the performance enhancement (PE) of the grooved inline and staggered microchannels with that of the smooth channel.

2. Problem Description

2.1 Mathematical Implementation

The LBM is called an alternative method to solve fluid flow and temperature transfer problems (Liao and Jen 2011. Fluid motion is driven by variations in temperature; therefore, it is very important to discuss thermal effects in conjunction with fluid flow. Therefore, many researchers have effectively used with different conditions the Thermal Lattice Boltzmann Method (TLBM) (Feng et al. 2018; Sahar

et al. 2017; Chai et al. 2008; Taher et al. 2017; Wan and Karniadakis 2006) to analyze the said problems.

A mesh unit is considered in LBM, depending on the motion of fluid particles, rather than directly resolving macroscopic fluid quantities such as pressure, velocity and temperature. As per the Boltzmann equation, it is recognized as a mesoscopic simulation model. Neglecting external forces, the discrete method for calculating momentum and energy in the Boltzmann equation can be stated as follows (Xu and Yan, 2023; Niu et al., 2007):

$$F_i(\vec{x}+\Delta t\vec{e}_i, t+\Delta t) - F_i(\vec{x},t) = -\frac{1}{\tau}\left[F_i(\vec{x}\,t) - F_i^{eiq}(\vec{x},t)\right] \quad (1)$$

$$G_i(\vec{x}+\Delta t\vec{e}_i, t+\Delta t) - G_i(\vec{x},t) = -\frac{1}{\tau_\theta}\left[G_i(\vec{x}\,t) - G_i^{eiq}(\vec{x},t)\right] \quad (2)$$

Where, $F_i(\vec{x},t)$ and $G_i(\vec{x},t)$ are defined as the momentum and energy distribution functions respectively. The relaxation time constant for momentum is denoted by τ and for energy indicated by τ_θ. The D2Q9 model, depicted by uniform Cartesian cells resembling a square lattice, is shown in Fig. 1.

There are 9 discrete velocities. Each time step involves the movement of particles from one node to another at a specific velocity. The lattice has three kinds of particles. There are 4 velocities which are moving along with the coordinate direction, the other 4 velocities are driven diagonally and one is at rest which is exists in the node.

$$e_i = \begin{cases} 0, & i=0 \\ \left(cos(\pi/4(i-1)), \sin(\pi/4(i-1))\right), & i=1,2,3,4 \\ \sqrt{2}\left(cos\left(\frac{\pi}{4(i-1)}\right), \sin(\pi/4(i-1))\right), & i=5,6,7,8 \end{cases}$$

With the help of lattice velocity, the momentum is F_i^{eq} and energy is G_i^{eq} can be written as (Rovenskaya and Croce, 2013):

$$F_i^{eq} = \rho\omega_i\left[1+\frac{3}{c^2}\vec{e}_i.\vec{u}^{eq}+\frac{9}{2c^4}(\vec{e}_i.\vec{u}^{eq})^2-\frac{3}{c^2}u^{eq^2}\right] \quad (3)$$

$$G_i^{eq} = \varepsilon\omega_i\left[1+\frac{3}{c^2}\vec{e}_i.\vec{u}^{eq}+\frac{9}{2c^4}(\vec{e}_i.\vec{u}^{eq})^2-\frac{3}{2c^2}u^{eq^2}\right] \quad (4)$$

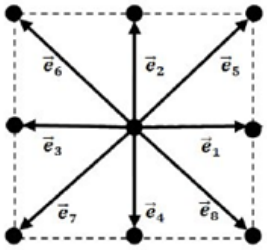

Fig. 1 Square Lattice D2Q9 model

The relaxation collation parameter for the temperature distribution function $\omega = \frac{1}{\tau}$ rely on the macroscopic variable quantity ρ and $\rho\vec{u}$. It should gratify the rules of conservation:

$$\rho = \sum_i F_i \text{ and } \rho\vec{u} = \sum_i \vec{e}_i F_i \quad (5)$$

It has been stated that the mentioned above equation successfully describes the Navier-Stokes equations for both temperature and velocity, as documented in (Xu and Yan, 2023; Liao and Jen, 2011; Chen and Tian, 2009). If (μ) represents the coefficient of viscosity and (K) denotes the thermal conductivity, this may be expressed as follows:

$$\mu = \left(\tau - \tfrac{1}{2}\right)\rho RT \text{ and } K = \left(\tau_\theta - \tfrac{1}{2}\right)\rho c_p RT \quad (6)$$

Indeed, in micro-flow systems, although the local concentration variation is minimal, it yields diverse effects. (Niu et al., 2007) integrated with a new relaxation time τ' rather than τ in equation (1) as follows

$$\tau' = \frac{1}{2} + \frac{1}{\rho}\left(\tau - \frac{1}{2}\right) \quad (7)$$

Given that the regenerative energy (ε) of the fluid mechanisms is represented as $\varepsilon(x,) = \sum_i G_i(x,\ t)$ and the internal energy (ε) is defined as $\varepsilon=\rho c_p T$, we can determine the average temperature of the fluid in these patterns as:

$$T = \frac{\varepsilon(x,t)}{\rho c_p} = \frac{\sum_i G_i(x,t)}{\rho c_p} \quad (8)$$

The study considers laminar flow in microchannel. Hence, investigating laminar flow within microchannels of varying roughness has become increasingly significant. Consequently, according to Liu et al. (2011), the ratio of Poiseuille number (Pn) and Reynolds number (Re) can be expressed as the friction factor (f). Thus, f can be expressed as:

$$f = \frac{\Delta pD}{\Delta L\frac{1}{2}(\rho)(u)^2} \quad (9)$$

Where, Δp, D, ΔL, ρ and u are pressure drop, the hydraulic diameter, channel length, density of the fluid and average velocity of the center line respectively. Where, $Re = \frac{\rho uD}{\mu}$. The following way is possible to write the Poiseuille number Pn:

$$Pn = fRe = \frac{\Delta pD}{\Delta L\frac{1}{2}\rho u^2} \times \frac{\rho uD}{\mu} = \frac{2\Delta p}{\Delta L}\frac{D^2}{\mu u} \quad (10)$$

The heat transfer rate is measured by the Nusselt number which can be notified as Nu. The dimensionless parameter of the heat transfer coefficients can be expressed by the following 14equation:

$$Nu = \frac{hL}{K} \tag{11}$$

Where, $h, L\ and\ K$ represented by the average convective heat transfer quantity per unit area, the thermal conductivity and the characteristics length respectively. Then, h can be defined as:

$$h = \frac{Q}{(\vec{T}_w - T_f)} \tag{12}$$

Q represents the convective heat transfer rate,

$$Q = mc_p(T_{mi} - T_{mo}) \tag{13}$$

T_{mi} denoted inlet temperature and T_{mo} identified outlet temperature. Additionally, the mean temperatures of the wall and the fluid are determined through the following calculations:

$$\overline{T_w} = \frac{1}{n}\sum_{i=1}^{n} T_{wi} \text{ and } T_f = \frac{\int_0^H uTdy}{\int_0^H udy} \tag{14}$$

A thermo-hydraulic performance parameter (η) or microchannel performance enhancement (PE) can be calculated as the ratio of the normalized heat transfer and friction coefficients. This parameter, also referred to as the coefficient of performance (COP), is articulated by (Yuan and Rahman, 2016; Rovenskaya and Croce, 2013) as follows:

$$PE = \frac{N^*}{(R^*)^{1/3}} \tag{15}$$

The normalized heat transfer coefficient N^* and the normalized friction coefficient R^* are defined by the following equations:

$$N^* = \frac{(N_u)_{rough}}{(N_u)_{smooth}}\ and\ R^* = \frac{(P_n)_{rough}}{(P_n)_{smooth}} \tag{16}$$

2.2 Geometry of the present problem

The geometry of the study is characterized by a horizontal microchannel in-line and staggered arrangement of roughness elements, called a grooved microchannel, is shown in (Fig. 2) Here, the height of the channel is represented by H, L denotes the channel, L/H=6. U, V, P_i and T_i denote the velocity, inlet pressure and temperature of the gas flow respectively. T_w indicates the wall temperature. The surfaces of the channel are isothermal and slippery. The relative roughness height is indicated by 'rh'. In the microchannel system, rh is estimated at rh=4%, 8% and 12%. The influence of rarefaction effects on microchannel performance could have a significant impact. When the channel length is significantly larger (L >> H) than the channel height, even in the small Reynolds number range, the Mach number can increase in pressure-driven gas flow due to the small hydraulic diameter and rapid pressure drop. (Xu and Yan, 2023; Rovenskaya and Croce, 2013).

The Reynolds number primarily depends onf the maximum flow velocity and hydraulic diameter of the channel, which should be less than 0.1*lu* times the characteristic length. Additionally, it is influenced by the fluid's conduction properties. To model laminar flow upstream in a microchannel, the maximum velocity U is considered at both the inlet and outlet locations, typically at the midpoint of the channel. The inlet Mach number should be below 0.3 to disregard compressibility effects. A pressure ratio conducted by $P_i/P_o = 1.10$. Mach number of 0.25, and Kn=0.02, 0.05, and 0.10, aiming to explore the highly small compressible condition (Boonloi and Jedsadaratanachai, 2022; Liu et al., 2011). The inlet and outlet of the fluid are assumed to be cold and the walls are heated uniformly.

The symbols σ and σ_T represent the tangential momentum and energy circumstance coefficients respectively. These coefficients play a vital role in determining the integral characteristics of wall boundaries, thus significantly influencing numerical outcomes. It's important to note that when the Knudsen number (Kn) remains constant, a

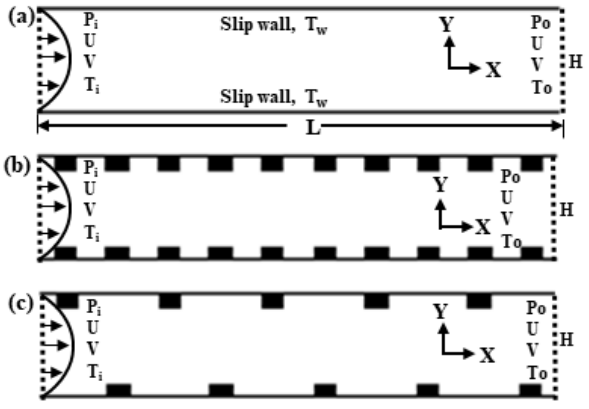

Fig. 2 Schematic of the geometry (a) smooth channel (b) in-line, and (c) staggered arrangement of grooved microchannels with boundary conditions.

decrease in thermal momentum (σ) increases wall slip. Alternatively, if σ stands constant, an growing in Kn leads to an rise in wall slip. A value of σ = 0 denotes a state of complete absence of friction at the wall, while a value of σ = 1 indicates adherence to a no-slip condition at the wall. (Taher et al., 2014, 2016; Chen and Tian, 2009).

In this study, the effects of Poiseuille number, operating pressure, inlet temperatures of the cold fluids, and wall thermal conductivity are investigated by a numerical method

Both mathematical and experimental results show that smooth microchannel walls lead to better performance when σ = 0.70 and rough wall boundary σ = 0.90 to 0.95 represents a higher result. D represents the hydraulic diameter which is computed among the inlet and outlet sections. For our present study, it is figured out for smooth microchannel $\sigma = \sigma_T = 0.70$ for rough microchannel $\sigma = \sigma_T = 0$. In this study, fluid properties are considered to be air properties where Pr=0.71. Calculations are made by the authors using a code in the FORTRAN language.

2.3 Code Validation

To validate this approach against the conventional benchmark, the friction factor fRe concerning the Poiseuille number (Pn) in a smooth microchannel at varying Knudsen numbers is illustrated in (Fig. 3). Using equation (10) the friction factor is calculated for the smooth channel at tangential momentum accommodation coefficient (TMAC), σ = 0.65 from Kn=0.02 to 0.10. The friction factor coefficient is degreasing regarding enhancement of the rarefaction effect as seen above in Fig. 3. At the wall boundary, indicates a high-velocity slip for increasing the Knudsen number. Figure 3 illustrates a strong correspondence between this study and the research conducted by (Liu et al., 2011).

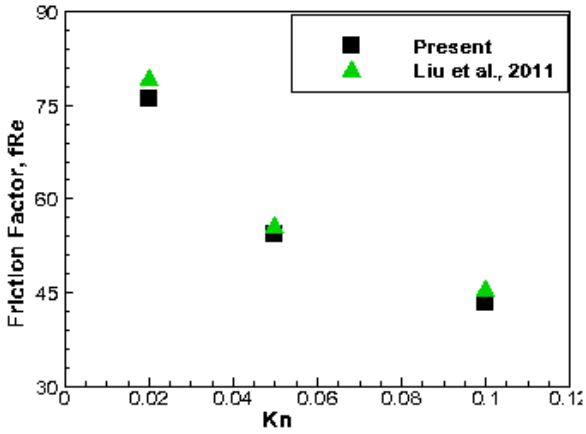

Fig. 3 Changes in the friction factor concerning the Poiseuille number are depicted across various Knudsen numbers (Kn) within a smooth channel.**3. Result and discussions**

3.1 Temperature Contour in Different Roughness Heights (rh) and Knudsen Number (Kn)

The TLBM is employed to solve equations (1) and (2) to obtain all expected outcomes. The study used a uniform 2D square lattice within the HPP model to address the boundary conditions and mathematical problems described above. According to dimensionless parameters, the numerical results are discussed in the area. The hydrodynamic parameters such as velocity, pressure, density, temperature etc. can be obtained regarding microscopic quantities such as momentum and energy distribution function. The variation of isotherms according to the temperature contours at the slip flow regime with roughness height is exhibited in (Figs 4-6).

The temperature contours demonstrate the temperature gradient near the heated corrugated surface due to mixing the working fluid with channel walls at the slip stream regime. The irregular motion of the fluid is caused by

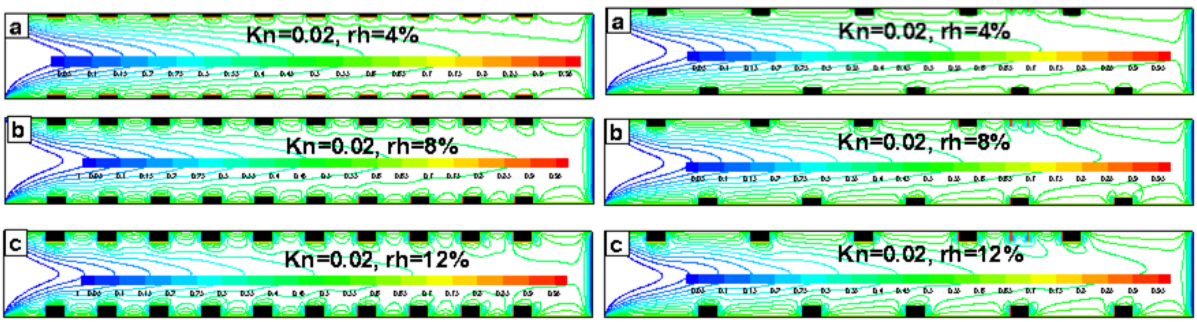

Fig. 4 Variations of the isotherms at Kn=0.02 with (a) rh=4%, (b) rh=8%, (c) rh=12% for in line (left) and staggered (right) grooved channel.

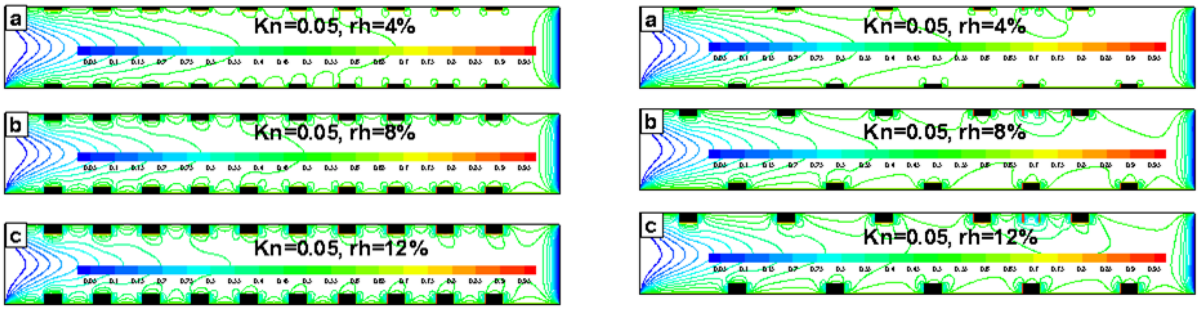

Fig. 5 Variations of the isotherms at Kn=0.05 with (a) rh=4%, (b) rh=8%, (c) rh=12% for inline (left) and staggered (right) grooved channel.

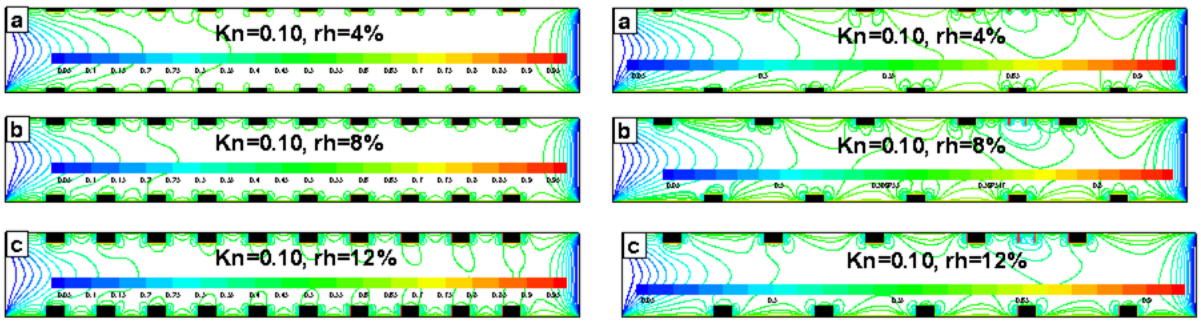

Fig. 6 Variations of the isotherms at Kn=0.10 with (a) rh=4%, (b) rh=8%, (c) rh=12% for inline (left) and staggered (right) grooved channel.

increasing the grooved height and therefore greater heat dissipation occurs inside the channel. From above (Figs. 4-6) fluids nearer to the wall have shown higher temperatures compared to the fluid flow of the channel at the center. Moreover, at the inlet section, the temperature contours displayed a symmetrical form and then with the effect of grooved, this symmetry is gradually lost especially for staggered grooved channels.

3.2 Streamlines in Terms of Velocity Vectors with Various Roughness Heights with Knudsen Number

Streamlines with velocity vectors regarding the height of the roughness at the slip flow management are shown in (Figs. 7-9). It is seen that the streamlines near the surface represented different characters of flow path due to the effect of arrangement as well as the height of the grooved. For larger roughness heights, vortices appeared on the front side and back side of the rectangular structures within the inline grooved microchannel, suggesting significant flow separation. Conversely, small vortices are observed at the rear of each rib in the staggered grooved microchannel. The presence of roughness elements leads to the expansion and contraction of streamlines near the rough surface, resulting in increased pressure drop and consequently higher friction.

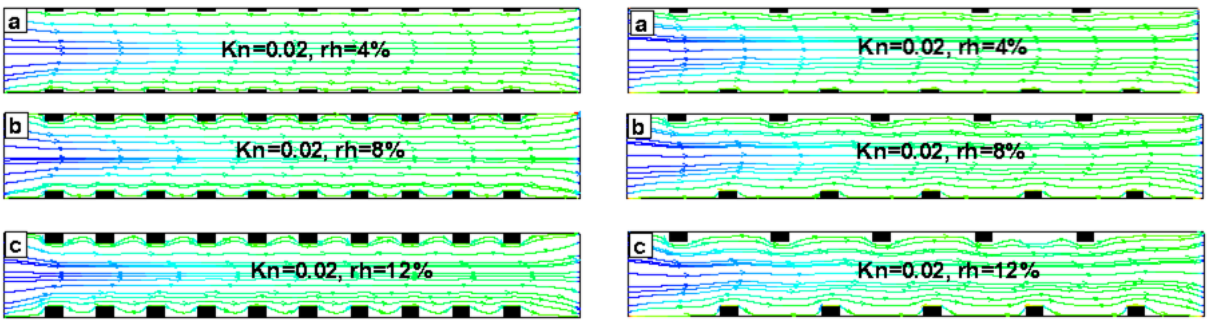

Fig. 7 Variations of the streamlines at Kn=0.02 with (a) rh=4%, (b) rh=8%, (c) rh=12% for inline (left) and staggered (right) grooved channel.

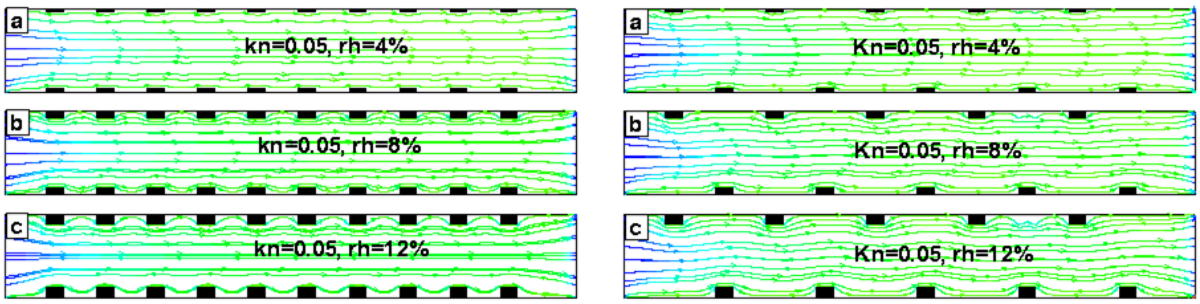

Fig. 8 Variations of the streamlines at Kn=0.05 with (a) rh=4%, (b) rh=8%, (c) rh=12% for inline (left) and staggered (right) grooved channel.

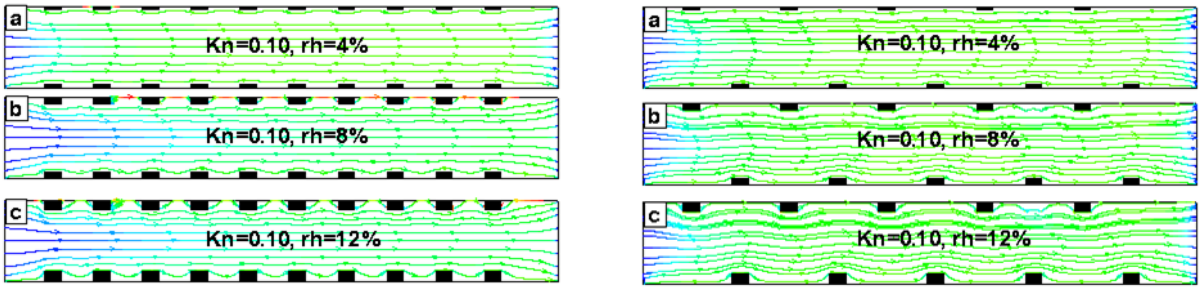

Fig. 9 Variations of the streamlines at Kn=0.10 with (a) rh=4%, (b) rh=8%, and (c) rh=12% for inline (left) and staggered (right) grooved channel.

3.3 U-velocity at Different Locations in Inline and Staggered Grooved Microchannel for Different Roughness Height (rh) with Knudsen Number (kn)

Figures 10-12 illustrate the U-velocity of inline and staggered grooved channels with different relative roughness heights (rh) at the locations *x*=0.6L and *x*=0.97L for different Kn=0.02 to 0.10. For the inline grooved channel, the velocity profiles have shown parabolic and maintained symmetrical properties throughout the channel. However, for the staggered grooved channel, the symmetry is gradually lost after the midsection of the channel, approximately when *x* is greater than 0.65L.

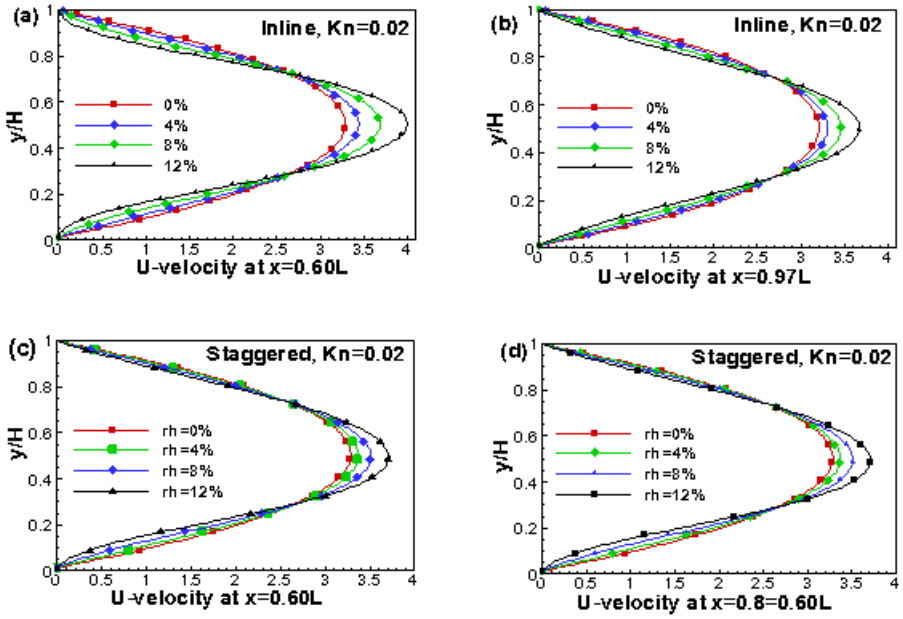

Fig. 10 U-velocity at different locations (*x*=0.6L and 0.97L) of inline (a)-(b) and staggered (c)-(d) grooved channels for different rh with Kn=0.02.

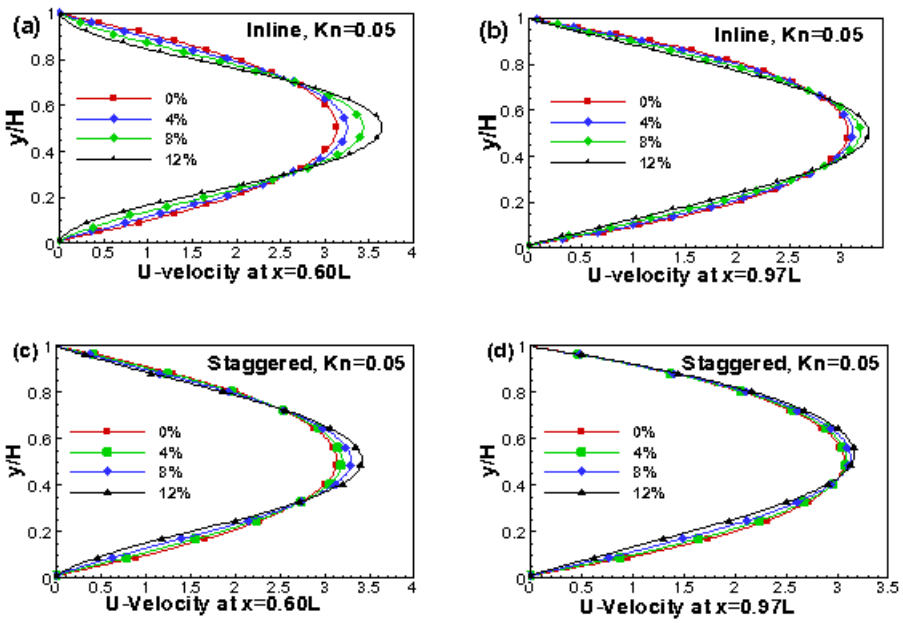

Fig. 11 U-velocity at different locations (x=0.6L and 0.97L) of inline (a)-(b) and staggered (c)- (d) grooved channel for various rh with Kn=0.05.

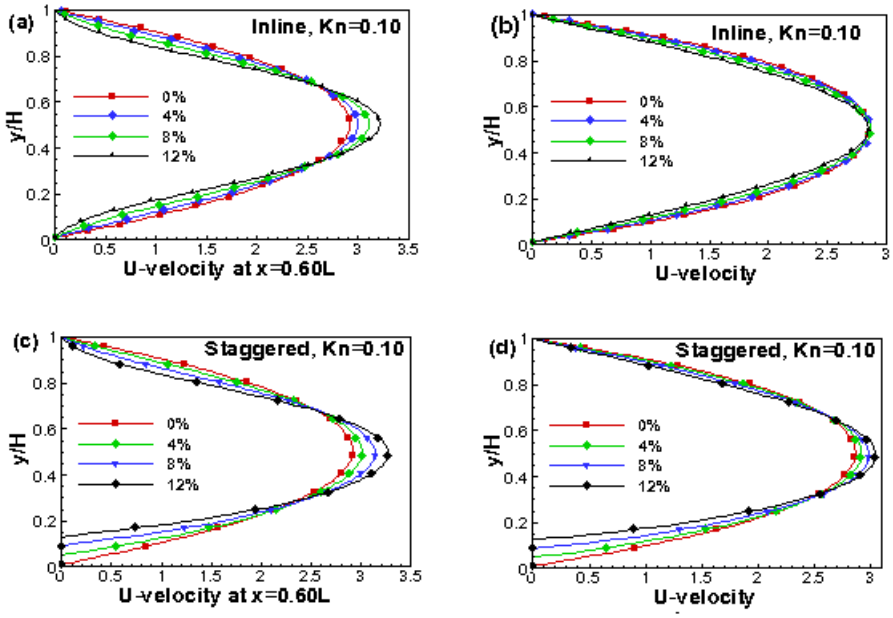

Fig. 12 U-velocity at different locations (*x*=0.6L and 0.97L) of inline (a)-(b) and staggered (c)-(d) grooved channels for different roughness heights with Kn=0.10.

3.4 Average Temperature Profiles with Different Roughness Heigh and Knudsen Numbers

The average temperature profiles with different roughness heights at the centerline of the grooved and staggered grooved channels for Kn=0.02, 0.05 and 0.10 are shown in (Figs. 13-14) As the walls are heated and cold fluid enters the channel, so fluid temperature increases throughout the channel due to fluid-solid interactions. The highest temperature is observed at the near end of the channel. The temperature increases with Kn but decreases with roughness height. Compared with inline, staggered and smooth microchannels the maximum temperature is shown in the smooth channel.

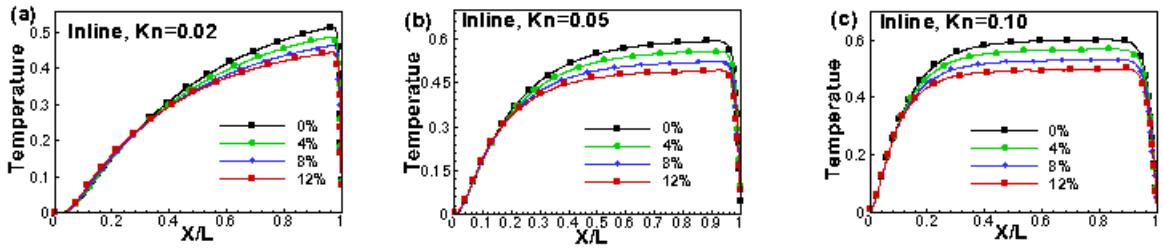

Fig. 13 Average temperature profiles at the centerline of the inline grooved channel for (a) Kn=0.02, (b) Kn=0.05 and (c) Kn=0.10 with different roughness heights.

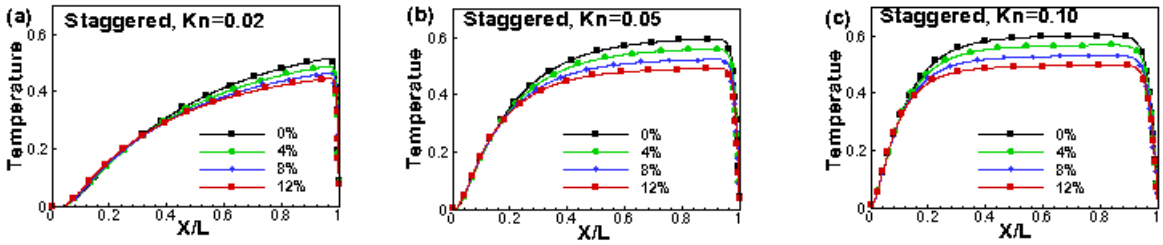

Fig. 14 Average temperature profiles at the centerline of the staggered grooved channel for (a) Kn=0.02, (b) Kn=0.05 and (c) Kn=0.10 with different rh.

3.5 Average Friction Coefficients with Different Knudsen Numbers and Relative Roughness Height

Flow friction, a form of resistance force that hampers or impedes motion, is important in numerous engineering contexts where, preventing sliding or slipping is paramount. For a comparison between smooth flow friction and inline and staggered grooved microchannels, the average friction coefficients are graphed in Figures 15 and 16

Figures 15-16 indicated that the average friction decreased significantly according to the increase for Kn= 0.02, 0.05 and 0.10. The bigger Knudsen number means the upper slippery between the wall and fluid particles and consequently less friction happened. However, the friction increased significantly with the increase of relative roughness height both for inline and staggered grooved channels. Furthermore, Figs. 15-16 illustrates that the maximum friction factor for an inline grooved microchannel is 107.053 when the lowest Knudsen number (Kn) is 0.02, with a roughness height (rh) of 12%. Moreover, the minimum average friction number is represented as 74.65 when the Knudsen number is 0.10 for a smooth channel. In addition, compared to smooth, inline and staggered channels, the lowest friction happened for smooth and the highest friction for inline grooved channels.

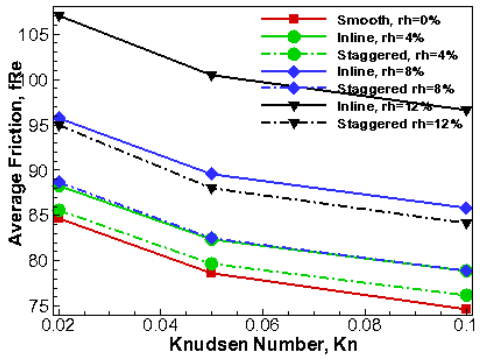

Fig. 15 The average friction for inline and staggered channels against the roughness heights for different Knudsen numbers (Kn)

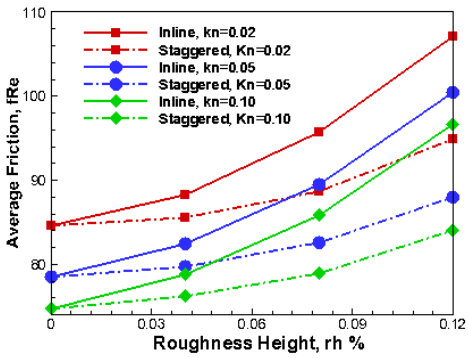

Fig. 16 The average friction for inline and staggered channels against the Knudsen numbers (Kn) for different roughness heights.

3.6 Heat Transfer Rate According to the Nusselt Number (Nu) Against the Various Roughness Height

The effect of roughness on heat transfer holds considerable importance in the design and operation of heat exchangers. This is especially notable where artificial roughness is employed to replicate distinctive and efficient heat transfer surfaces.

To investigate the thermal conductivity in smooth, inline, and staggered grooved microchannels, Figures 17-18 present the Nusselt numbers across various roughness heights and Knudsen numbers (Kn). As the Knudsen number and relative roughness height increase, the heat transfer rate decreases significantly in both inline and staggered grooved microchannels. In addition, Figs. 17-18 illustrate that the maximum heat transfer rate is 9.015 for a Knudsen number (Kn) of 0.02 with a smooth microchannel, while the minimum heat transfer rate, at 0.569, occurs for a Knudsen number of 0.10 with rh=12%. The staggered grooved microchannel exhibits a greater heat transfer rate compared to the inline case, with a pronounced difference observed particularly at lower Knudsen numbers, notably for Kn=0.02.

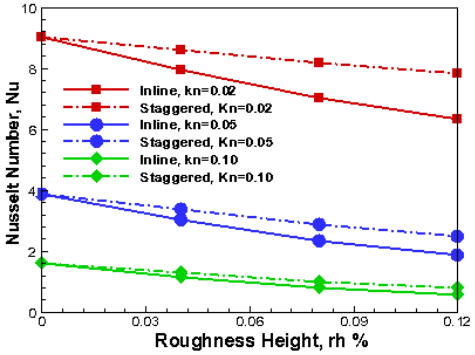

Fig. 17 The rate of heat transfer regarding Nu for inline and staggered channels in terms of Kn for different rh.

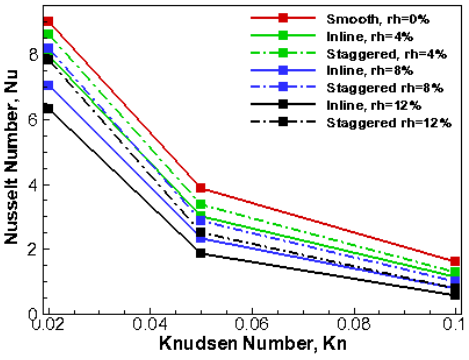

Fig. 18 The rate of heat transfer regarding Kn for inline and staggered channels in terms of Nu for different rh

3.7 Performance Analysis Compare to Different Knudsen Numbers and Roughness Height

This study has investigated the thermal-hydraulic performance of inline and staggered roughness geometries, recognizing the importance of simultaneously calculating heat transfer and flow friction. This is particularly relevant in MEMS (Micro-Electro-Mechanical Systems) devices due to their practical applications:

Figure 19 displayed the performance enhancement (PE) of the microchannel designed against rh for Kn values of 0.02, 0.05, and 0.10 within the slip flow regime. Both the increasing roughness height and Knudsen number lead to a reduction in the fluid's performance. Specifically, the fluid's performance decreases with rising roughness height, and this trend is consistent across different Knudsen numbers. Higher slip and higher roughness height indicate lower performances in all cases. Moreover, the maximum performance is observed for a smooth microchannel which is the unity. This is because the pressure drop is minimum in the smooth channel. Moreover, Fig. 19 show that the maximum performance for staggered microchannels is PE=1.00, 0.950458, 0.894475, and 1.013248 for different roughness heights, rh=0%, 4%, 8%, and 12% respectively, with Kn=0.02. Compared to the inline grooved channel, the staggered grooved microchannel demonstrates better performance. This is because the pressure drop was the lowest in the trapezoidal channel compared. This kind of research has both scientific interest and technological impact and it might be applied to the design and optimization of MEMS devices.

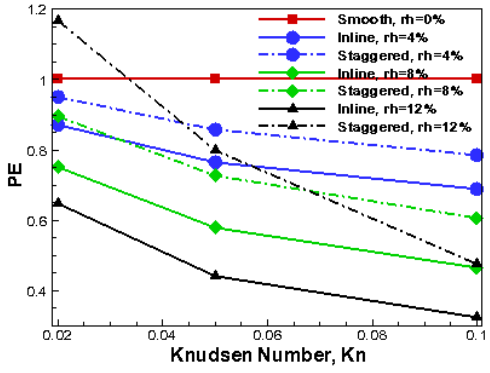

Fig. 19 The performance enhancement for inline and staggered channels against the roughness heights for various Kn.

4. Conclusions

The TLBM is fruitfully applied in this investigation to examine the thermal and fluid flow behaviors at the slip flow regimes. This investigation considers different Kn=0.02, 0.05, and 0.10) in both inline and staggered grooved microchannels. The surface roughness elements are rectangular, with relative roughness heights ranging from 4%, 8%, to 12%. The following are the key observations from this study:

- Streamlines near the surface represented different characters of flow path due to the effect of arrangement regarding the height of the grooved.
- The temperature gradually enhancement with Kn but decreases with roughness height. For all cases, the maximum temperature is shown of smooth channels.
- The average friction decreased linearly with increasing the Knudsen numbers (Kn) and increased significantly with the increase of relative roughness height both for inline and staggered grooved channels. In addition, compared to smooth, inline and staggered channels, the lowest friction happened for smooth and the highest friction for inline grooved channels.
- The Nusselt number (Nu) according to heat transfer rate is significantly decreased with both cases of increasing Knudsen number and growing roughness height. However, the staggered grooved channel case, represents the greater heat transfer amount related to the inline case and the change is noticeable for the lower Knudsen number.

The thermal-hydraulic performance namely the performance enhancement decreases both for increasing roughness height with Knudsen number. The maximum performance is exhibited for smooth microchannel. But, compared to the inline grooved channel, the staggered grooved microchannel has shown better performance.

Future Work:

The study may be extended by considering the following cases:

- To investigate fluid flow and heat transfer inline and staggered with entry and exit length effect.
- To study with various types of roughness element with regular and irregular arrangements on walls.
- To examine rough microchannel heat transfer enhancement with nanofluid using LBM.

References

Abdelsalam, S. I., A. M. Alsharif, Y. Abd Elmaboud, A. I. Abdellateef (2023). Assorted kerosene-based nanofluid across a dual-zone vertical annulus with electroosmosis. Heliyon, 9(5): e15916. https://doi.org/10.1016/j.heliyon.2023.e15916

Abdelsalam, S. I., A. Z. Zaher (2023). Biomimetic amelioration of zirconium nanoparticles on a rigid substrate over viscous slime—a physiological approach. Applied Mathematics and Mechanics, 44(9): 1563-1576. https://doi.org/10.1007/s10483-023-3030-7

Aouissi, Z., Chabane, F., Teguia, M. S., Bensahal, D., Moummi, N., & Brima, A. (2023). Numerical and experimental investigations of heat transfer inside a rectangular channel with a new tilt angle of baffles for solar air heater. Journal of Renewable Energy and Technology, 1, 9-15. https://doi.org/10.38208/jret.v1i1.376

Bhatti, M. M., K. Vafai, S. I. Abdelsalam (2023). The role of nanofluids in renewable energy engineering. Nanomaterials, 13(19): 2671. https://doi.org/10.3390/nano13192671

Biswas, S., P. Sharma, B. Mondal, G. Biswas (2015). Analysis of mixed convective heat transfer in a ribbed channel using the lattice Boltzmann method. Numerical Heat Transfer, Part A: Applications, 68(1): 75-98. https://doi.org/10.1080/10407782.2014.965095

Boonloi, A., W. Jedsadaratanachai (2022). Effects of Baffle Height and Baffle Location on Heat Transfer and Flow Profiles in a Baffled Duct: A CFD Analysis. Modelling and Simulation in Engineering, 2022: 698887. https://doi.org/10.1155/2022/3698887

Cao, B. Y., M. Chen, Z. Y. Guo (2006). Effect of surface roughness on gas flow in microchannels by molecular dynamics simulation. International Journal of Engineering Science. 44(13-14): 927-937. https://doi.org/10.1016/j.ijengsci.2006.06.005

Chai, Z., Z. Guo, L. Zheng, B. Shi (2008). Lattice Boltzmann simulation of surface roughness effect on gaseous flow in a microchannel. Journal of Applied Physics. 104(1): 014902. https://doi.org/10.1063/1.2949273

Chen S., Z. Tian (2009). Simulation of microchannel flow using the lattice Boltzmann method. Physica A: Statistical Mechanics and its Applications. 388(23): 4803-4810. https://doi.org/10.1016/j.physa.2009.08.015

Dahani, Y., A. M. Amahmid, Hasnaoui, S. Hasnaoui, A. El Mansouri, I. Filahi (2023). Thermal boundary conditions at the fluid–solid interface in the case of a conducting body: a novel thermal lattice Boltzmann analysis. Thermophysics and Aeromechanics, 30(5): 865-892. https://doi.org/10.1134/S0869864323050062

D'Orazio, A., M. Corcione, G. P. Celata (2004). Application to natural convection enclosed flows of a lattice Boltzmann BGK model coupled with a general-purpose thermal boundary condition. International Journal of Thermal Sciences, 43(6): 575-586. https://doi.org/10.1016/j.ijthermalsci.2003.11.002

Fábregas, J., H. Santamaria, E. Buelvas, S. Perez, C. Díaz, J. Carpintero, R Mendoza, J. Villa (2022). Computational fluid dynamics modeling of microchannels cooling for electronic microdevices. IIUM Engineering Journal, 23(1): 384-396. https://doi.org/10.31436/iiumej.v23i1.2113

Feng, Y. L., S. L. Guo, W. Q. Tao, P. Sagaut (2018). Regularized thermal lattice Boltzmann method for natural convection with large temperature differences. International Journal of Heat and Mass Transfer, 125: 1379-1391. https://doi.org/10.1016/j.ijheatmasstransfer.2018.05.051

Harris, M., H. Wu, W. Zhang, A. Angelopoulou (2022). Overview of recent trends in microchannels for heat transfer and thermal management applications. Chemical Engineering and Processing-Process Intensification, 181: 109155. https://doi.org/10.1016/j.cep.2022.109155

He, X., S. Chen, G. D. Doolen (1998). A novel thermal model for the lattice Boltzmann method in incompressible limit. Journal of computational physics, 146(1): 282-300. https://doi.org/10.1006/jcph.1998.6057

Jafari, S. M., S. S. Jabari D., Dehnad, S. A. Shahidi (2017). Heat transfer enhancement in thermal processing of tomato juice by application of nanofluids. Food and Bioprocess Technology, 10: 307-316. https://doi.org/10.1007/s11947-016-1816-9

Ji, Y., K. Yuan, J. N. Chung (2006). Numerical simulation of wall roughness on gaseous flow and heat transfer in a microchannel. International journal of heat and mass transfer, 49(7-8): 1329-1339. https://doi.org/10.1016/j.ijheatmasstransfer.2005.10.011

Kim, S. H., H. Pitsch, I. D. Boyd (2008). Slip velocity and Knudsen layer in the lattice Boltzmann method for microscale flows. Physical review E. 77(2): 026704. https://doi.org/10.1103/PhysRevE.77.026704

Liao, Q., T. C. Jen (2011). Application of Lattice Boltzmann method in fluid flow and heat transfer. Computational Fluid Dynamics Technologies and Applications. 29-68. https://doi.org/10.5772/10585

Liu, C., J. Yang, Y. Ni (2011). A multiplicative decomposition of Poiseuille number on rarefaction and roughness by lattice Boltzmann simulation. Computers & Mathematics with Applications. 61(12): 3528-3536. https://doi.org/10.1016/j.camwa.2010.03.030

Mohamad, A. A. (2007). Applied lattice Boltzmann method for transport phenomena, momentum, heat and mass transfer. Canadian Journal of Chemical Engineering. 85(6): 946-946. https://doi.org/10.1002/cjce.5450850617

Niu, X. D., C. Shu, Y. T. Chew (2007). A thermal lattice Boltzmann model with diffuse scattering boundary condition for micro thermal flows. Computers & Fluids. 36(2): 273-281. https://doi.org/10.1016/j.compfluid.2005.11.007

Qi, C., C. Li, K., Li D., Han (2022). Natural convection of nanofluids in solar energy collectors based on a two-phase lattice Boltzmann model. Journal of Thermal Analysis and Calorimetry, 147: 2417–2438. https://doi.org/10.1007/s10973-021-10668-8

Rovenskaya, O. I., G. Croce (2016). Numerical simulation of gas flow in rough microchannels: hybrid kinetic–continuum approach versus Navier–Stokes. Microfluidics and Nanofluidics, 20: 1-15. https://doi.org/10.1007/s10404-016-1746-x

Rovenskaya, O., G. Croce (2013). Numerical investigation of microflow over rough surfaces: coupling approach. Journal of heat transfer. 135(10): 101005. https://doi.org/10.1115/1.4024500

Sahar, A. M., J. Wissink, M. M. Mahmoud, T. G. Karayiannis, M. S. A. Ishak (2017). Effect of hydraulic diameter and aspect ratio on single phase flow and heat transfer in a rectangular Karayiannis's microchannel. Applied Thermal Engineering, 115: 793-814. https://doi.org/10.1016/j.applthermaleng.2017.01.018

Sharma, A. K., P. S. Mahapatra, N. K. Manna, K. Ghosh (2015). Mixed convection in a baffled grooved channel. Sadhana. 40: 835-849. https://doi.org/10.1080/10407782.2014.955359

Taher, M. A., D. MK, L. YW (2017). Effects of surface roughness on thermal and hydrodynamic behaviors in microchannel using lattice Boltzmann method. International Journal of Fluid Machinery and Systems. 10(4): 439-446. https://doi.org/10.5293/IJFMS.2017.10.4.439

Taher, M. A., H. D. Kim, Y. W. Lee (2014). LBM simulation on friction and mass flow analysis in a rough microchannel. Journal of Advanced Marine Engineering and Technology, 38(10): 1237-1243. https://doi.org/10.5916/jkosme.2014.38.10.1237

Taher, M. A., H. D. Kim, Y. W. Lee (2015). Study of thermal and hydraulic performances of circular and square ribbed rough microchannels using LBM. Journal of Thermal Science. 24: 549-556. https://doi.org/10.1007/s11630-015-0821-z

Taher, M. A., Y. W. Lee, H. D. Kim (2016). LBM simulation on natural convection flows in a triangular enclosure of greenhouse under winter day conditions. Journal of Engineering Thermophysics, 25: 411-423. https://doi.org/10.1134/S1810232816030103

Taher, M. A., M. M. R. Liton, R. Biswas, P. Chakma, Y. W. Lee (2022a). Numerical analysis of thermal and flow friction in lid-driven grooved enclosure using Lattice Boltzmann Method. Journal of Advanced Marine Engineering and Technology (JAMET). 46(1): 23-30. https://doi.org/10.5916/jamet.2022.46.1.23

Tan, Z., H. Yan, R. Huang, L. Liu, Q. Li (2022b). Phase-field lattice Boltzmann method for the simulation of gas-liquid mass transfer. Chemical Engineering Science, 253: 117539. https://doi.org/10.1016/j.ces.2022.117539

Walter, C., S. Martens, C. Zander, C. Mehring, U. Nieken (2020). Heat transfer through wire cloth micro heat exchanger. Energies, 13(14): 3567. https://doi.org/10.3390/en13143567

Wan, X., G. E. Karniadakis (2006). Stochastic heat transfer enhancement in a grooved channel. Journal of Fluid Mechanics. 565: 255-278. https://doi.org/10.1017/S0022112006001819

Wang, C. S., P. Y. Shen, T. M. Liou (2020). A consistent thermal lattice Boltzmann method for heat transfer in arbitrary combinations of solid, fluid, and porous media. Computer Methods in Applied Mechanics and Engineering. 368: 113200. https://doi.org/10.1016/j.cma.2020.113200

Xu, W., G. Yan (2023). A lattice Boltzmann model for the Navier-Stokes equation. Microprocessors and Microsystems, 96: 104391. https://doi.org/10.1016/j.micpro.2021.104391

Yuan, Y., S. Rahman (2016). Extended application of lattice Boltzmann method to rarefied gas flow in micro-channels. Physica A: Statistical Mechanics and its Applications, 463: 25-36. https://doi.org/10.1016/j.physa.2016.06.123

Zhang, G., B. Liu, A. Xu, Y. Y. ShanLi (2019). Morphology effect of surface structures on microchannel flow using lattice Boltzmann method. Geofluids, 2019(1): 3475872. https://doi.org/10.1155/2019/3475872

Zhao, Y. L., Z. M. Wang (2019). Lattice Boltzmann simulation of micro gas flows over a wide range of Knudsen numbers. Journal of Fluids Engineering. 141(9): 091401. https://doi.org/10.1115/1.4042886

Zhu, Q., K. Chang, J. Chen, X. Zhang, H. Xia, H. Zhang, Y. Jin (2020). Characteristics of heat transfer and fluid flow in microchannel heat sinks with rectangular grooves and different shaped ribs. Alexandria Engineering Journal. 59(6): 4593-4609. https://doi.org/10.1016/j.aej.2020.08.014